doi:10.1016/j.jmb.2009.07.061 J. Mol. Biol. (2009) 392, 868–871

JMB

Available online at www.sciencedirect.com

ScienceDirect

ELSEVIER

COMMUNICATION

Imaging Amyloid Fibrils within Cells Using a Se-Labelling Strategy

Alexandra E. Porter[1]*, Tuomas P. J. Knowles[2], Karin Muller[3], Sarah Meehan[4], Eva McGuire[1], Jeremy Skepper[3], Mark E. Welland[2] and Christopher M. Dobson[4]*

[1]*Department of Materials, Imperial College London, London SW7 2AZ, UK*

[2]*Nanoscience Centre, University of Cambridge, J. J. Thomson Avenue, Cambridge CB3 0FF, UK*

[3]*Department of Physiology, Development and Neuroscience, University of Cambridge, Cambridge CB2 3DY, UK*

[4]*Department of Chemistry, University of Cambridge, Lensfield Road, Cambridge CB2 1EW, UK*

Received 18 April 2009; received in revised form 13 July 2009; accepted 21 July 2009
Available online 25 July 2009

Edited by J. Weissman

The process of aggregation leading to amyloid formation by peptides and proteins is associated with diseases ranging from systemic amyloidoses to neurodegenerative disorders such as Alzheimer's disease. A key question in understanding the link between amyloid formation and its pathological consequences is the ultrastructural localisation and morphological form of amyloid species within the cellular environment. The acquisition of such information has proven to be challenging, but we report here a novel approach that enables amyloid fibrils to be visualised directly within a cell. First, fibrils are assembled from selenium analogues of the sulfur-containing cysteine peptides, and then, atomic number contrast transmission electron microscopy is used to detect the selenium doped species selectively within the carbon-rich background of the cell. We demonstrate the power of this approach by imaging human monocyte-derived macrophage cells that have been exposed to fibrils from an amyloidogenic fragment of the disease-associated protein transthyretin. The ready incorporation of seleno-cysteine and methionine instead of their natural sulfur-containing analogues, a feature that is already commonly used in X-ray diffraction studies of proteins, suggests that this method can be used as a general strategy to image specific peptides and proteins within the cellular environment using electron microscopy.

Keywords: amyloidosis; neurodegenerative disorders; seleno-amino acids; human macrophage cell; electron microscopy

The transitions of peptides and proteins from their soluble, native, biologically active structures into intractable polymeric assemblies[1,2] are events that underlie a multitude of disorders, including many with high socioeconomic impact such as Alzheimer's and Parkinson's diseases and late-onset diabetes.[1,3,4] Although recent research has revealed increasingly detailed molecular events associated with the formation of such aggregates,[5–8] the localisation of these structures within the cell and the detailed mechanisms that characterise their involvement in disease states are crucial questions that largely remain to be addressed.[8] The challenges in providing answers to such question originate from difficulties in imaging carbon-containing polypeptide aggregates within the carbon-rich cell.[9] Traditional electron microscopy techniques address the contrast problem by staining thin, resin-embedded sections with agents that enhance electron scattering such as heavy metal salts;[10] in many cases, however, the low level of specificity of such staining procedures seriously limits its application for the identification of specific aberrant species such as protein aggregates within the cell in a reliable manner.[11]

In this article, we describe an alternative approach for increasing selectively the contrast of intracellular

**Corresponding authors.* E-mail addresses: a.porter@imperial.ac.uk; cmd44@cam.ac.uk.

Abbreviations used: STEM, scanning transmission electron microscopy; HAADF, high-angle annular dark field; EDX, energy dispersive X-ray spectroscopy; 3-D, three-dimensional.

peptide aggregates by labelling the fibrils in such a way as to increase their scattering power relative to other assemblies in the cell. Rather than relying on a potentially intrusive chemical marker substance, however, we have incorporated the seleno-analogue of the sulfur-containing amino acid cysteine, which possesses a larger electron scattering cross section than its natural counterpart but is chemically essentially identical with it. Indeed, this exact substitution approach has revolutionised X-ray diffraction studies involving proteins by enabling the phase problem to be solved through multi-wavelength anomalous diffraction.[12–14] Here, we show that we can exploit the electron scattering properties of selenium with scanning transmission electron microscopy (STEM). By using a high-angle annular dark field (HAADF) detector, which collects electrons that undergo Rutherford scattering, we found out that the intensity in the resulting images is approximately proportional to the square of the atomic number of the scattering atoms Z.[15–17] This technique is consequently highly sensitive to local variations in the atomic number within the sample, a key feature underlying the present selective imaging approach.

We first generated amyloid fibrils from a peptide corresponding to residues 10–19 of human transthyretin,[18] a protein associated with systemic amyloid diseases such as familial amyloid polyneuropathy, familial amyloid cardiopathy, and senile systemic amyloidosis, and from an analogous peptide in which the cysteine residue in position 10 is replaced by its seleno-analogue. Fibril formation was achieved by incubating the peptides for periods up to 4 weeks at a concentration of 10 mg/ml at 37 °C in a solution of 10% acetonitrile in water (v/v) adjusted to pH 2.0 with HCl.[19] For electron microscopy studies, we exposed human monocyte-derived macrophage cells to the fibrils for 3 days at concentrations of 125 μg/ml, according to a protocol published previously.[20] Following this procedure, the viability of the cells exposed to fibrils was measured relative to unexposed cells using the neutral red assay; no evidence of a significant decrease in cell viability was observed after 3 days of exposure to 125 μg/ml of fibrils. The washed cell

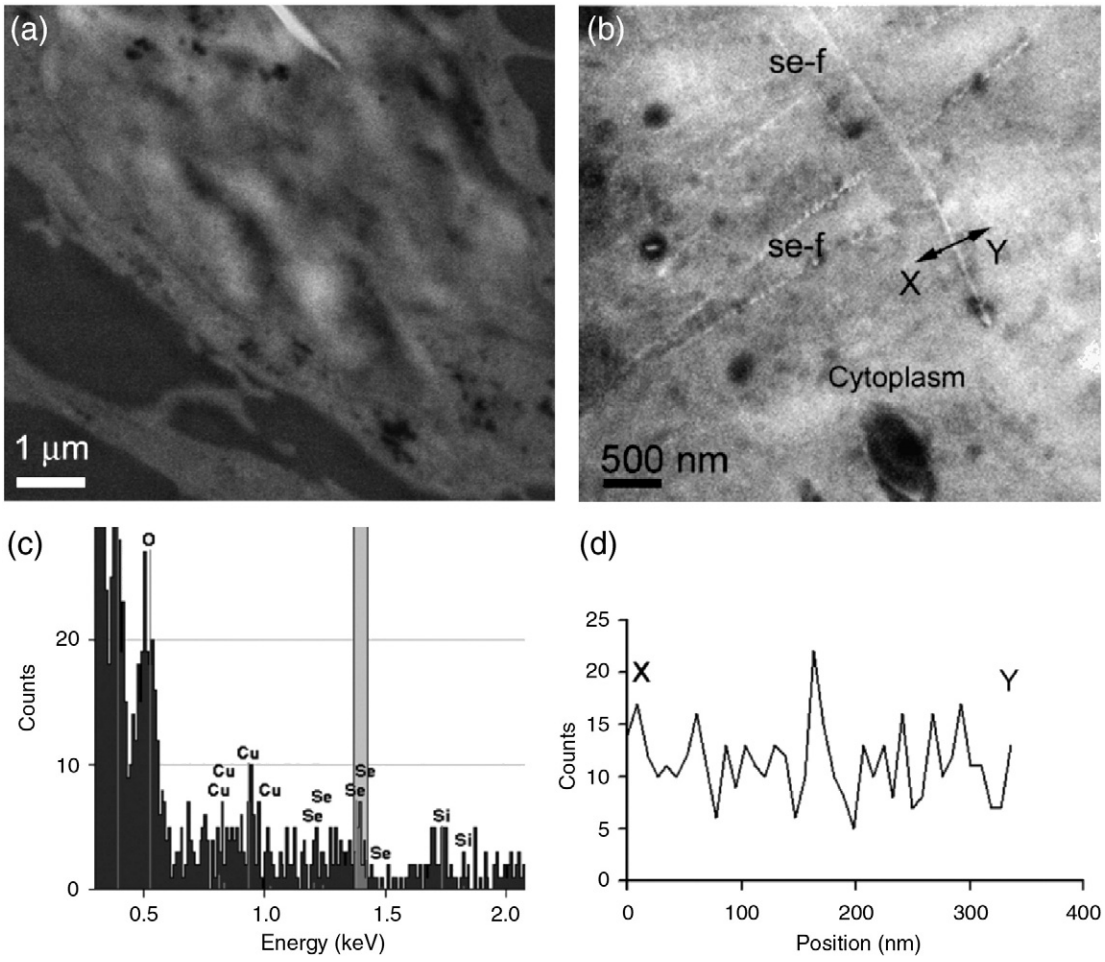

Fig. 1. (a) HAADF-STEM images of human monocyte-derived macrophage cells exposed to unlabelled TTR fibrils, showing a lack of detectable contrast from the fibrils. (b) Se-labelled peptide fibrils (se-f) within the cytoplasm. (c) EDX spectra from the peptide within the cell in (b). The tall grey bar has been used to highlight the selenium peak and represents the energy window used to form the line profile in (d). (d) Selenium EDX intensity profile across x–y in (b), with increased intensity co-localised with the fibrils, demonstrating that the Se signal originates from the labelled fibrils.

layers were then fixed with 4% glutaraldehyde in Pipes buffer (0.1 M, pH 7.4) for 1 h and then treated successively for 5 min with graded aqueous solutions of ethanol (70%, 95%, and 100% v/v alcohol). Samples were infiltrated under vacuum with Quetol resin (Agar Scientific, UK) for 3 days and then cured in fresh Quetol resin for 24 h at 60 °C.

The cells exposed to fibrils were then cut into sections of 40 nm thickness with an ultramicrotome and mounted onto 600-mesh bare copper grids. No formvar or carbon support films were used in order to minimise incoherent scattering of electrons and, hence, to enhance contrast. All TEM observations were then made by analyzing several areas from multiple specimens. HAADF-STEM combined with energy dispersive X-ray spectroscopy (EDX) experiments were performed on an FEI-F20 Tecnai microscope operating at 200 kV using a 30-mm condenser aperture and a camera length of 200 mm. The principle underlying the operation of EDX is the detection of X-rays that are produced when the electron beam is accelerated onto the sample. The electron beam excites the atoms in the sample that subsequently produce X-rays with discrete energies that are different for every element. The number and energy of the X-rays emitted from the specimen are then measured by a detector recording an energy spectrum of intensity *versus* energy. The characteristic energy distribution in the spectrum provides information about the composition of the sample being studied, and the intensity of the peaks provides information about the amount of each element present in the sample.

In these experiments, the unlabelled peptide fibrils could not be observed within the cell (Fig. 1a); however, contrast from the Se fibrils could be seen clearly within the cytoplasm of the cell (Fig. 1b), highlighting the dramatic effects of the heavy element labels on the species of interest. In order to confirm that the origin of the enhanced scattering was the presence of the selenium atoms incorporated into the fibrils, we measured EDX line profiles across the fibril images as shown in Fig. 1d; the energy spectra of the resulting emitted photons indicate clearly the presence of selenium (Fig. 1c). Furthermore, the highest concentration of selenium coincides with the highest electron scattering as observed in the HAADF-STEM images (Fig. 1b and d). The characteristic signature of selenium in the EDX spectrum enables us, therefore, to pinpoint specifically the location of the labelled species. Indeed, the contrast in the fibril images shown in Fig. 1b is even greater than might be expected from the intensity of the selenium peak in Fig. 1c as a result of mass thickness effects that arise because the fibrillar aggregates are denser than the cell cytoplasm.

We next performed three-dimensional (3-D) electron tomography on selected sections of cells exposed to the Se peptide in order to visualise the distribution of protein aggregates in three dimensions; HAADF-STEM tomographic data sets were acquired over a tilt range of −70 to +70 using a step size of 2 in order to achieve this objective. For these measurements, we used samples of 200 nm thickness in order to increase volume information for 3-D tomography. 3-D reconstruction was carried out using the simultaneous iterative reconstruction technique[21,22] using EMISPEC 3-D reconstruction software; reconstructed images were visualised in slices using Amira™ 3D visualization software (Mercury Computer Systems Inc., Merignac Cedex, France). Figure 2a shows a projection image for which a Voltex 3D reconstruction method reveals that the fibrils are intracellular; that is, they had entered the cell from the external medium. Furthermore, the reconstructions (Fig. 2b) suggest that the Se fibrils could cluster together within a membrane-bound compartment, such as a lysosome into which species targeted by the cell for degradation are trafficked.[23–25] The difference in distribution and bundling of fibrils in Figs. 1 and 2 suggests more than one pathway into the cell.

In conclusion, the results of this study show that the use of peptides in which natural sulfur atoms are

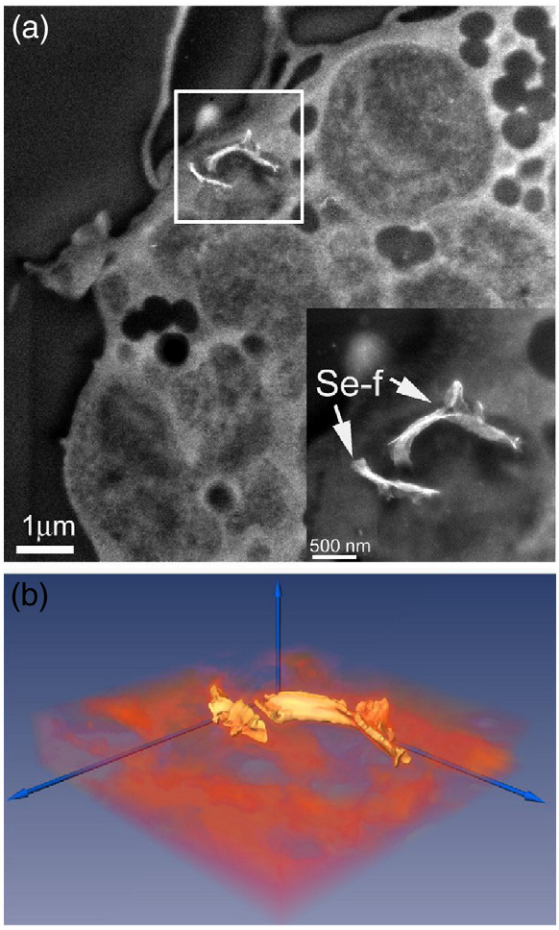

Fig. 2. Electron tomography experiments showing the presence of clusters of Se peptide fibrils in the lysosomes of the cell. (a) Zero-tilt projection image. Inset from boxed region showing a higher magnification image of the Se peptide fibrils within a lysosome. (b) Voltex projection of the 3-D reconstruction of (a) with isosurface rendered Se peptide structures shown in gold and the cytoplasm in orange.

replaced by selenium atoms enables the observation of amyloid fibrils within individual cells and cell compartments. This approach therefore represents a powerful tool for future investigations of the molecular processes that underlie the normal and aberrant effects of protein self-assembly and misassembly in living systems, particularly with the remarkable developments that have occurred recently in the field of electron tomography.[26,27] More generally, the success of this approach suggests that it can be used more widely to identify and locate other specific proteinaceous components in cells. The strategy described here is then of particular interest as a wide variety of chemical and molecular biology techniques exist for the incorporation of selenium either as a replacement for sulfur or through the incorporation of nonnatural amino acids during protein synthesis.[28]

Acknowledgements

Financial support was provided by the Interdisciplinary Research Collaboration in Nanotechnology, the Isaac Newton Trust, the Engineering and Physical Sciences Research Council, the FEI Company, the Royal Academy of Engineering, the Oppenheimer Research Trust, and St. John's College, Cambridge. The Multiimaging Centre was established with funding from the Wellcome Trust. The research of C.M.D. is supported in part by the Wellcome and Leverhulme Trusts.

References

1. Chiti, F. & Dobson, C. M. (2006). Protein misfolding, functional amyloid, and human disease. *Annu. Rev. Biochem.* **75**, 333.
2. Dobson, C. M. (2003). Protein folding and misfolding. *Nature*, **426**, 884.
3. Pepys, M. B. (2001). Pathogenesis, diagnosis and treatment of systemic amyloidosis. *Philos. Trans. R. Soc. London, Ser. B*, **356**, 203.
4. Kelly, J. W. (2002). Towards an understanding of amyloidogenesis. *Nat. Struct. Biol.* **9**, 323.
5. Hardy, J. & Selkoe, D. J. (2002). The amyloid hypothesis of Alzheimer's disease: progress and problems on the road to therapeutic. *Science*, **297**, 353.
6. Jarrett, J. T. & Lansbury, P. T. (1993). Seeding "one-dimensional crystallization" of amyloid—a pathogenic mechanism in Alzheimer's disease and scrapie? *Cell*, **736**, 1055.
7. Rochet, J. C. & Lansbury, P. T. (2000). Amyloid fibrillogenesis: themes and variations. *Curr. Opin. Struct. Biol.* **10**, 60.
8. Lansbury, P. T. & Lashuel, H. A. (2006). A century-old debate on protein aggregation and neurodegeneration enters the clinic. *Nature*, **443**, 774.
9. Jensen, G. J. (2009). Cell biology. Protein filaments caught in the act.. *Science*, **323**, 472.
10. Hardwick, S. J., Hegyi, L., Clare, K., Law, N. S., Carpenter, K. L., Mitchinson, M. J. & Skepper, J. N. (1996). Apoptosis in human monocyte-macrophages exposed to oxidized low density lipoprotein. *J. Pathol.* **179**, 294.
11. Robinson, C. V., Sali, A. & Baumeister, W. (2007). The molecular sociology of the cell. *Nature*, **450**, 973.
12. Hendrickson, W. A., Pähler, A., Smith, J. L., Satow, Y., Merritt, E. A. & Phizackerley, R. P. (1989). Crystal structure of core streptavidin determined from multiwavelength anomalous diffraction of synchrotron radiation. *Proc. Natl Acad. Sci. USA*, **86**, 2190.
13. Pahler, A., Smith, J. & Hendrickson, W. (1990). A probability representation for phase information from multiwavelength anomalous dispersion. *Acta Crystallogr., Sect. A: Found. Crystallogr.* **46**, 537.
14. Hendrickson, W. A. (1985). Analysis of protein structure from diffraction measurement at multiple wavelengths. *Trans. Am. Crystallogr. Assoc.* **21**, 11.
15. James, R. W. (1948). *The Crystalline State.* Bell & Hyman, Ltd., London.
16. Treacy, M. M. J. & Howie, A. J. (1980). Contrast effects in the transmission electron microscopy of supported crystalline catalyst particles. *J. Catal.* **63**, 265.
17. Howie, A. (1979). Electron microscope image contrast and localized signal selection techniques. *J. Microsc.* **117**, 11.
18. Gustavsson, A., Engström, U. & Westermark, P. (1991). Normal transthyretin and synthetic transthyretin fragments form amyloid-like fibrils in vitro. *Biochem. Biophys. Res. Commun.* **175**, 1159.
19. MacPhee, C. E. & Dobson, C. M. (2000). Formation of mixed fibrils demonstrates the generic nature and potential utility of amyloid nanostructures. *J. Am. Chem. Soc*, **122**, 12707.
20. Porter, A. E., Muller, K., Skepper, J., Midgley, P. & Welland, M. (2006). Uptake of C60 by human monocyte macrophages, its localization and implications for toxicity: studied by high resolution electron microscopy and electron tomography. *Acta Biomater.* **2**, 409.
21. Kak, A. C. & Slaney, M. (1988). *Principles of Computed Tomography Imaging*. IEEE, Piscataway, NJ.
22. Gilbert, P. (1972). Iterative methods for the three-dimensional reconstruction of an object from projections. *J. Theor. Biol.* **36**, 105.
23. Duve, C. D. & Wattiaux, R. (1966). Functions of lysosomes. *Annu. Rev. Physiol.* **28**, 435.
24. Hershko, A. & Ciechanover, A. (1982). Mechanisms of intracellular protein breakdown. *Annu. Rev. Biochem.* **51**, 335.
25. de Duve, C. (2005). The lysosome turns fifty. *Nat. Cell Biol.* **7**, 847.
26. Beck, M., Luci, V., Förster, F., Baumeister, W. & Medalia, O. (2007). Snapshots of nuclear pore complexes in action captured by cryo-electron tomography. *Nature*, **449**, 611.
27. Brandt, F., Etchells, S. A., Ortiz, J. O., Elcock, A. H., Hartl, F. U. & Baumeister, W. (2009). The native 3D organization of bacterial polysomes. *Cell*, **136**, 261.
28. Noren, C. J., Anthony-Cahill, S. J., Griffith, M. C. & Schultz, P. G. (1989). A general method for site-specific incorporation of unnatural amino acids into proteins. *Science*, **244**, 182.